Tunable THz Generation by the Interaction of a Super-luminous Laser Pulse with Biased Semiconductor Plasma

K. Papadopoulos[1,2] and A. Zigler[1,3]

[1]*BAE Systems-ATI*
[2]*University of Maryland, College Park MD 20742 USA*
[2]*Hebrew University*

Abstract. Terahertz (THz) radiation is electromagnetic radiation in the range between several hundred and a few thousand GHz. It covers the gap between fast-wave electronics (millimeter waves) and optics (infrared). This spectral region offers enormous potential for detection of explosives and chemical/biological agents, non-destructive testing of non-metallic structural materials and coatings of aircraft structures, medical imaging, bio-sensing of DNA stretching modes and high-altitude secure communications. The development of these applications has been hindered by the lack of powerful, tunable THz sources with controlled waveform. The need for such sources is accentuated by the strong, but selective absorption of THz radiation during transmission through air with high vapor content. The majority of the current experimental work relies on time-domain spectroscopy using fast electrically biased photo-conductive sources in conjunction with femto-second mode-locked Ti:Sapphire lasers. These sources known as Large Aperture Photoconductive Antennas (LAPA) have very limited tunability, relatively low upper bound of power and no bandwidth control. The paper presents a novel source of THz radiation known as *Miniature Photoconductive Capacitor Array* (*MPCA*). Experiments demonstrated tunability between .1 – 2 THz, control of the relative bandwidth $\Delta f/f$ between .5-.01, and controlled pulse length and pulse waveform (temporal shape, chirp, pulse-to-pulse modulation *etc*.). Direct scaling from the current device indicates efficiency in excess of 30% at 1 THz with $1/f^2$ scaling at higher frequencies, peak power of 100 kW and average power between .1-1 W. The physics underlying the *MPCA* is the interaction of a super-luminous ionization front generated by the oblique incidence of a Ti:Sapphire laser pulse on a semiconductor crystal (ZnSe) biased with an alternating electrostatic field, similar to that of a frozen wave generator. It is shown theoretically and experimentally that the interaction results in the emission of an electromagnetic wave at the plasma frequency of the ionization front. The device resembles the well-known *DARC* plasma device [1] with two significant differences. First, the frozen wave is on a semiconductor crystal and not on a gas (Azulene Vapor). Second, the ionizing front is super-luminous. These differences result in a device with superior tunability, efficiency, compactness and flexibility. The paper concludes with examples of THz imaging using the *MPCA*.

Keywords: Tunable Terahertz Source.

CP807, *High Energy Density and High Power RF: 7th Workshop,* edited by D. K. Abe and G. S. Nusinovich

OVERVIEW

Terahertz (THz), as the name implies, refers to frequencies in the region of 1000 GHz. It forms the boundary between high-speed electronics and optics. It is usually known as the frequency gap between millimeter wave technology, extending up to about 100 GHz (0.1 THz), and middle infra-red electro-optic technology which extends down to about 10 THz (Fig. 1) and is characterized by a lack of tunable sources with significant power.

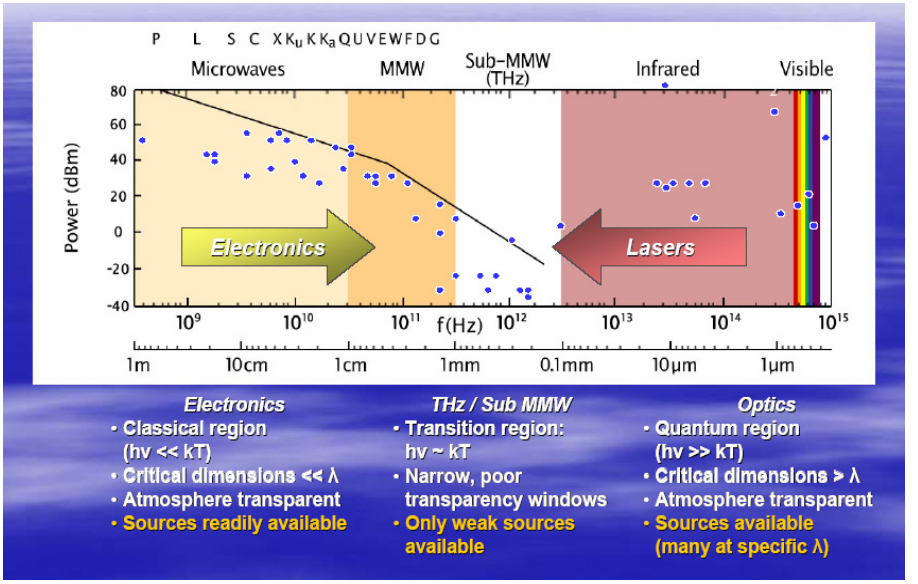

FIGURE 1. Illustration of the THz gap.

Interest in this spectral region arises from both curiosity about the last unexplored region of electromagnetic spectrum and from potential applications including radar, medical imaging, secure communications and the detection of explosives and chemical/biological agents. For example, radars operating at THz frequencies have much higher angular resolution than existing millimeter wave systems resulting in improved image resolution. The potential of THz waves to penetrate non-metallic materials, such as clothing and cardboard packaging, opens the door to applications in the security field for detecting concealed weapons like guns or explosives. THz frequencies cover the rotational and vibrational absorption bands of molecules and spectra measured as a result of interaction of THz radiation with complex materials provide information on the chemical composition as well as the three-dimensional structure of target objects. This has applications in materials research, in the medical field, and in nondestructive testing of non-metallic materials such a structural fiber composites and ceramics. Furthermore, it can characterize targets, and improve discrimination between soft and hard objects.

Application of THz radiation has been hampered in the past by a number of technological issues, most importantly:

1. a lack of powerful, tunable THz radiation sources (Fig. 1);
2. the absence of sensitive, fast, portable, non-cryogenic detectors;
3. difficulties in propagating THz radiation through standard atmospheric conditions; especially in high humidity.

The last item places a heavy burden on the type of sources required for field applications of THz radiation, as can be seen by reviewing briefly the propagation of THz radiation through the atmosphere. Atmospheric propagation at THz frequencies is strongly affected by water vapor absorption. For frequencies higher than 2 THz the absorption is great enough to prevent transmission over more than a few meters at sea level. However, the absorption rate is significantly reduced between 0.1-1.5 THz and above 12 THz. Kilometer ranges can be obtained for frequencies in between absorption peaks. Water vapor content varies quite a lot with geographical location and with the time of year. As an example, the low-frequency THz transmission over a 30 m path for mid-latitude summer and winter conditions obtained using the HINTRAN 2000 data-base is shown in Fig. 2. In winter the temperature is lower, so the water vapor content of the atmosphere is less, and the THz transmission is considerably greater. In the tropics, the humidity is generally higher, so transmission is less. It is clear that a powerful, tunable source with a tunable bandwidth is an absolute requirement, especially for field applications.

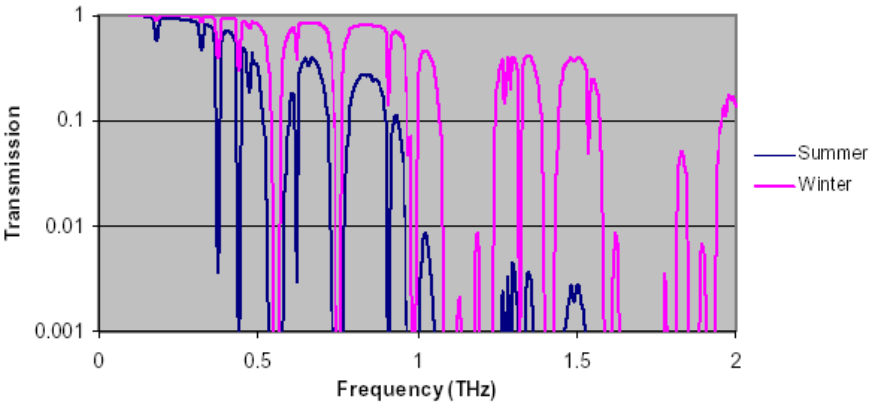

FIGURE 2. Atmospheric transmission at THz frequencies over a 30 m path for mid-latitude summer and winter conditions. Water vapor content content=1.88% vol. (summer) and .432% vol. (winter).

SOURCES OF THZ RADIATION

As illustrated in Fig. 1 one can approach the THz generation either from below, using either direct generation by micro-machined vacuum tubes or electronic up-conversion, or from above, using photonic down-conversion. Despite significant progress on all of the above, sources based on these ideas are still inadequate in power,

bandwidth or tunability in fulfilling the requirements for field applications. More promise has been shown by techniques that rely on the interaction of recently developed ultra-short pulse (femto-second) lasers with semiconductor crystals. Femto-second pulses generated by commercially available bench-top mode-locked lasers, interact with biased ultra-fast photoconductors to yield current transients with significant power in THz frequencies. Attaching these to miniature dipole radiators produces broadband radiation that can be collimated into a narrow beam by parabolic mirrors. This THz radiation concept is based on the principle of the Austin switch [2] illustrated in Fig. 3.

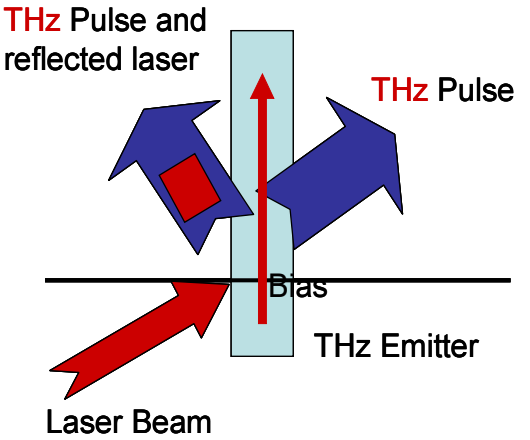

FIGURE 3. Austin switch concept for THz generation.

A conceptually interesting device, utilizing a short pulse laser and an electrically-biased medium, generated tunable microwave radiation between 20 and 60 GHz with a controlled bandwidth [1,3]. The principle of the device, known as a "DC to AC Radiation Converter" or DARC, is illustrated in Fig. 4. A capacitor array with alternating voltages is immersed into a neutral gas with low ionization potential and pressure in the few millitorr range (*e.g.* azulene or TMA). A 50 ps, 30 mJ pulse from a UV laser (λ = 266 nm) incident upon the DARC device creates a relativistic ionization front. Each time the front crosses a capacitor, it triggers a burst of current and, consequently, a burst of broadband radiation. The bursts generated from each capacitor sum coherently with a phase determined by the front velocity to produce an electromagnetic (EM) radiation pulse in the plasma with a particular frequency and propagation direction. The energy carried by the EM pulse is taken from the electrostatic energy of the capacitor array. The laser pulse energy is used for the ionization of the working gas only. The frequency of the EM pulse is tunable by adjusting either the plasma density – *i.e.*, the working gas pressure prior to ionization – or the capacitor spacing *d*. Details of the device as well as proof-of-principle experiments can be found in [1]. In addressing the suitability of the DARC device for THz generation we find that the major problem lies in the relatively large ionization potential of the gas (6-10 eV) relative to the allowable pre-ionization voltage, since the number of carriers increases as the square of the emitted frequency. This restricts the

practical utility of the DARC device to frequencies lower than 100 GHz, unless a more efficient ionization concept such as field ionization is implemented [4].

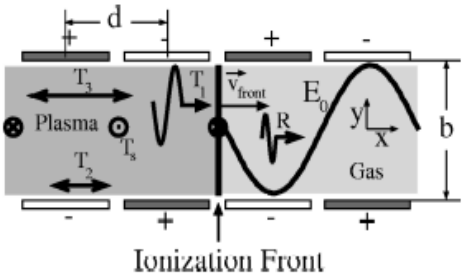

FIGURE 4. Geometry of DARC source. The static electric field of the capacitor array is converted into frequency tunable radiation upon transmission through the radiation front. The radiation pulse (T_1) follows the ionization front. Other excited modes include the reflected mode (R), two plasma modes (T_2 and T_3) and a free streaming mode (T_s) [1].

THE MINIATURE PHOTOCONDUCTIVE CAPACITOR ARRAY (MPCA)

Device Physics

The MPCA source described is a hybrid source that combines attributes from Large Aperture Photoconductive Antennas (LAPA) and DARC. It utilizes a capacitor array similar to DARC but is inserted in a semiconducting crystal (ZnSe in the case described below) rather than a neutral gas and uses a semiconductor crystal and oblique laser incidence similar to LAPA. The result, as will be demonstrated below theoretically and experimentally, is a more flexible, efficient, and powerful device than either.The principle of operation of the MPCA is illustrated in Fig. 5. A biased capacitor array similar to DARC is filled with a ZnSe crystal. It is illuminated by a femto-second Ti:Sapphire laser at an oblique angle θ and thus generates a super-luminous ionization front. The carrier generation is accomplished by two-photon absorption. The subsequent THz generation physics is similar to DARC with the exception that the bursts of radiation associated with capacitor discharge move at super-luminous speed and the coherent addition occurs at the plasma frequency ω determined by two conditions [5]: (*i*) the plasma dispersion relation and (*ii*) the continuity conditions at the boundary. The dispersion relation is

$$kc/\omega = \sqrt{\varepsilon}\,\{1-(\omega_e^2/\omega^2)\,[\omega/(\omega-i\gamma)]\}^{1/2} \qquad (1)$$

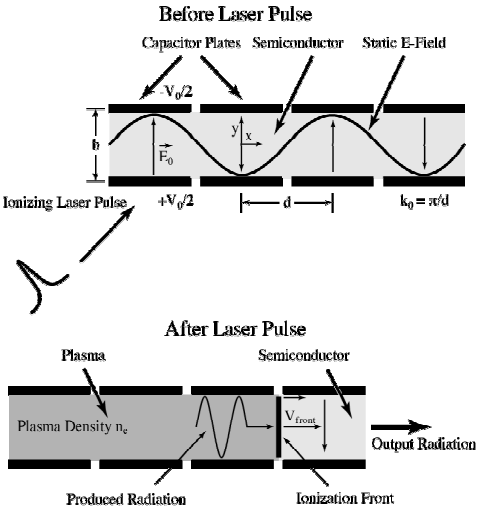

FIGURE 5. Principle of operation of the MPCA. A femto-second laser pulse incident obliquely on the device generates an ionization moving at superluminous speed c/β resulting in coherent radiation at the plasma frequency.

where ε is the dielectric constant of the semiconductor, ω_e is the plasma frequency and γ is a phenomenological de-phasing rate. The phase of the "frozen wave" is $\pm k_o z$, while the phase of the transmitted wave, which represents the tunable radiation, is $\omega t + kz$. Equating these and using $z = v_F t$, where $v_F = c/\sin\theta$ and θ is the incidence angle of the laser on the semiconductor, we find

$$k_o c/\sin\theta = \omega + kc/\sin\theta \qquad (2)$$

The emission frequency ω is given by the solution of (1) and (2). Defining $\beta = 1/\sin\theta$ and for $\omega_e >> \gamma$ and the trivially satisfied condition $\varepsilon^2\beta^2 >> 1$, ω is given by

$$\omega = \frac{k_o c}{\varepsilon\beta}[1 + (\varepsilon^2\beta^2)(\frac{ne^2}{\varepsilon m^* k_o^2 c^2})]^{1/2} \qquad (3)$$

It is easy to see that in the absence of plasma, *i.e.* $\omega_e \rightarrow 0$ or $\omega >> \omega_e$, (3) reduces to the frozen generator case. On the other hand, for $\varepsilon^2\beta^2 >> 1$, (3) gives

$$\omega = \omega_e = (n\, e^2/\varepsilon\, m^*)^{1/2} \qquad (4)$$

In this regime of operation of the MPCA, the radiation frequency is only a function of the semiconductor carrier density, which in turn is only a function of the energy in the ionizing laser pulse.

We should emphasize that the above analysis depends on the validity of the dispersion relation given by (1). This requires that the absorption depth δ of the laser

in the semiconductor exceeds c/ω_e ($\delta >> c/\omega_e$). Otherwise, the plasma will not support collective volume plasma modes. In the MPCA device, this is accomplished by relying on two-photon absorption. In this case, $\delta \approx 1/(\alpha I)$, where I is the laser intensity and α the two-photon absorption coefficient. The plasma density n is given by

$$n = \alpha W^2/h\nu S^2\tau \tag{5}$$

In (5), W is the laser energy per pulse, ν and τ the laser frequency and pulse length, respectively, and S is the illuminated area of the crystal. Combining (4) and (5) we find that

$$\omega \propto W / S \tag{6}$$

The two-photon absorption is a physics requirement of the concept. A one photon absorption such as used for LAPA generates semiconductor plasmas of thicknesses smaller than c/ω_e, where ω_e is the plasma frequency of the mobile carriers. Such plasmas do not support the coherent volume plasma modes. Equation (6) shows an essential feature of the MPCA: it indicates that the center frequency of the emitted radiation can be tuned by changing the incident laser fluence.

The second essential feature of the MPCA is the bandwidth control. This is accomplished by controlling the number N of active capacitors in the MPCA array. With an array of N capacitors, the output pulse is $N/2$ cycles long. For a laser pulse length $\tau=N\pi/\omega$, the expected bandwidth is given by

$$\Delta\omega/\omega \approx 2/N \tag{7}$$

Controlling the number of active capacitors controls the bandwidth of the radiation.

Proof-of-Principle Experiment

A proof-of principle experiment of the MPCA was conducted to test the theoretical predictions [5-9]. The experimental setup is shown in Fig. 6. It has three components: the electrically-biased radiating structure (based on a ZnSe photo-conductor), a Ti-Sapphire 100 fs laser, and a radiation detector. The ZnSe crystal was placed between the two thin glass plates with a multiple electrode structure made by evaporation of an aluminum structure on the plates. The capacitor plates were 3 mm by 10 mm, separated by a distance of 3 mm giving d = 6 mm. The capacitor plates were extended over the crystal to create a uniform field inside the crystal. The capacitors were alternately biased with a voltage between 50-120 volts to form a frozen wave configuration**.** In the absence of collective plasma effects (*i.e.* for $\omega >> \omega_e$) the device would generate frequency $\pi c/d$ = 2.5 GHz. Our experiments were performed for frequencies in excess of 100 GHz.

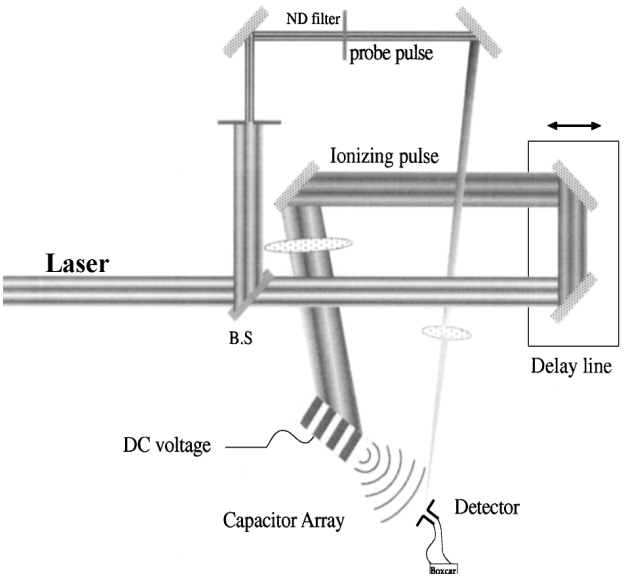

FIGURE 6. Experimental configuration using shoot-and-probe detection.

The radiation was generated by sweeping a 100 fs laser pulse from a Ti:Sapphire laser operating at 0.8 μm wavelength, with the energy per pulse limited to 2 mJ, and with a repetition rate of 10 Hz. The pulse was projected at an oblique angle of incidence on the crystal. The waveform of the radiated electric field was measured using the standard pump and probe technique: the laser beam was split into two beams, with the main beam, carrying more than 90% of the energy, serving as the pump beam and the second beam serving as the probe beam.

The propagating ionizing front was formed by focusing the main beam with a cylindrical lens on the side of the crystal. The crystal was placed at 20 degree angle with respect to the pump laser beam front. The amplitude of radiated electric field was monitored by a gated planar dipole antenna. The dipole antenna was constructed on a heavy ion implanted silicon layer on a sapphire substrate, which resulted in a sub-picosecond temporal response due to the short recombination time. The antenna detector was gated with different delays by varying the optical delay between the pump and probe laser pulses. The maximum frequency response of the configuration was approximately 2 THz, dictated by the carrier lifetime of the dipole antenna (<.5 psec). The profile of the radiated electric field was determined by monitoring the average current versus the time delay between the pump laser beam and the probe laser beam.

The first test gave a confirmation of the scaling of the emitted THz frequency with the laser intensity. This is shown in Fig. 7. The figure shows the measured emission central frequency as a function of the laser pulse energy W, in the range between 0.1 and 1 mJ, for constant illumination. The experimental points were derived following

the procedure outlined above. It is clear that the frequency of the radiation scales linearly with the energy in the laser pulse as predicted by (6).

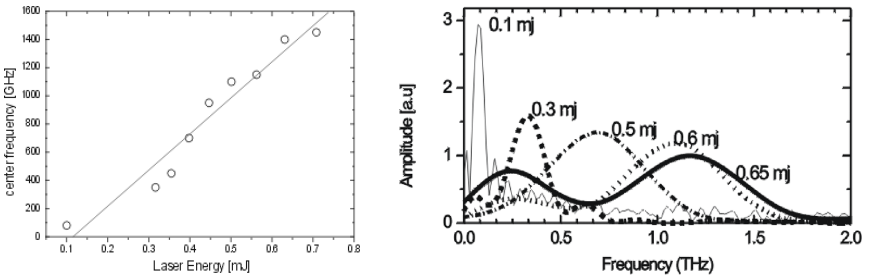

FIGURE 7. Emitted frequency as a function of laser fluence.

The second test was control of the radiation bandwidth. This was accomplished by controlling the number of charged capacitors in the structure. A typical measured temporal scan of the emitted radiation electric field and its power spectrum is shown in Fig. 8. The scan represents the measured signal intensity versus the delay between the pump and the probe laser pulse. Figure 8 (upper left) is for $W = 0.3$ mJ and a single capacitor, $N = 1$. Figure 8 (lower left) corresponds to $W = 0.35$ mJ and $N = 10$. That the narrowing of the spectrum from $\Delta\omega/\omega \approx 1$ to 0.1 is consistent with (7) is clearly seen, as is the shifting of the central frequency by 15%. Figure 8 (right) shows control of spectral width for a frequency close to 0.4 THz.

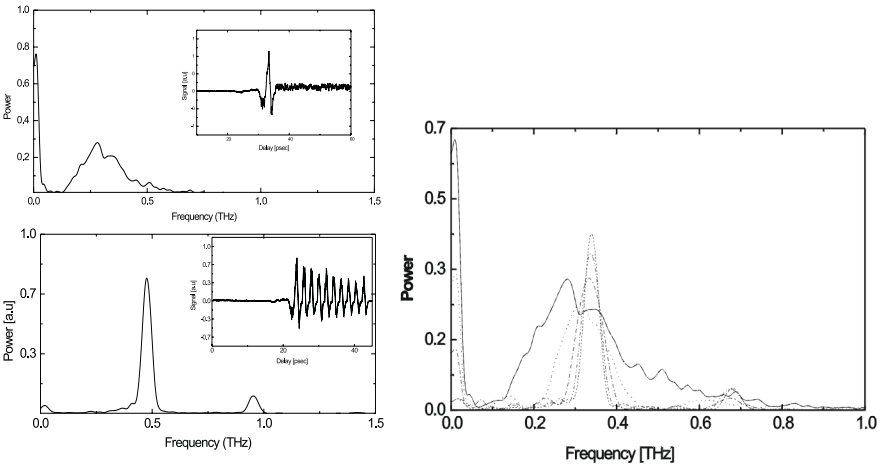

FIGURE 8. Generation of broadband (upper left) and narrowband (lower left) radiation and control of spectral width for the same central frequency (right).

The final test concerns scaling of the THz output power with the energy stored in the capacitor array. For a constant configuration, we expect that the signal amplitude will scale with the charging voltage as confirmed in Fig. 9.

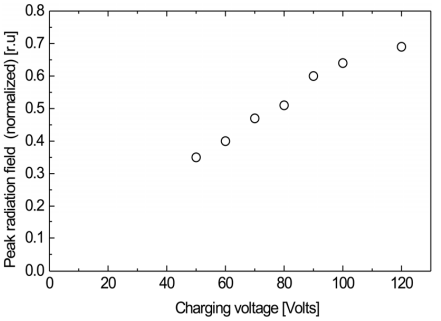

FIGURE 9. Scaling of the relative peak radiation field with charging voltage.

CONCLUDING REMARKS

In this paper we presented a proof-of-principle experiment along with a discussion of the underlying physics a novel THz source. It was shown that the MPCA can be tuned by controlling the incident laser fluence. Furthermore, the spectral width of the output can be controlled by changing the number of active capacitors in the array. A number of other features that have been demonstrated and not presented here include modulation capability and bandwidth control using a switchboard concept. The conversion efficiency of the MPCA is a subject of current study. It was shown above that the output power scales with the maximum allowable voltage; this in its turn depends on the breakdown field of the crystal. In the current low budget proof-of-principle experiment, the charging voltage gave electric field values of 1-2 kV/cm that were consistent with flashover limits. However, by carefully packaging the array in vacuum or imbedding it in an oil bath one can achieve fields limited by volume breakdown limits. Experiments have shown charging voltages that correspond to 120 kV/cm for ZnSe illuminated with two-photon absorption. Conversion efficiency on the order of 10% or better is expected depending on the radiated frequency. Using diamond crystal with a breakdown field limit of 1 MV/cm can provide a highly efficient THz source, at expense of requiring a UV laser. These issues are currently under study and will be reported later.

ACKNOWLEDGMENTS

The authors are indebted to Drs. T. Wallace, J. Sentfle and R. Shanny for a number of discussions concerning MPCA and its applications. This work was supported by BAE Systems –ATI IR&D.

REFERENCES

1. P. Muggli, R. Liou, C.H. Lai, J. Hoffman, T.C. Katsouleas and C. Joshi, *Physics of Plasmas* **5**, 2112 (1998).
2. M. P. Brown and K. Austin, *Appl. Phys. Letters* **85**, 2503-2504 (2004).
3. W.B. Mori, T. Katsouleas, J.M. Dawson and C.H. Lai, *Phys. Rev. Lett.* **74**, 544 (1995).

4. T. Katsouleas, private communication (2005).
5. D. Hashimshony, A. Zigler and K. Papadopoulos, *Phys. Rev. Lett*. **86**, 2806 (2001).
6. D. Hashimshony, A.Zigler and K. Papadopoulos, *Appl. Phys. Lett*.**75**, 892, (1999).
7. D. Hashimshony**,** A. Zigler and K. Papadopoulos, *Rev. of Scientific Instruments*, **71**, 2380, (2000).
8. A. Zigler, D. Hashimshony, and K. Papadopoulos, *IEEP- Optoelectron*. **149 (3**), 93, (2002).
9. D. Hashimshony, A. Zigler and K. Papadopoulos, *Photonics,* edited by R.J. Hwu and K. Wu, *Proc. SPIE*, 477, (1999).